THE JOURNAL OF BIOLOGICAL CHEMISTRY
Vol. 277, No. 51, Issue of December 20, pp. 49523–49530, 2002

Printed in U.S.A.

Cytotoxic Cell Granule-mediated Apoptosis

CHARACTERIZATION OF THE MACROMOLECULAR COMPLEX OF GRANZYME B WITH SERGLYCIN*

Received for publication, September 19, 2002, and in revised form, October 15, 2002
Published, JBC Papers in Press, October 17, 2002, DOI 10.1074/jbc.M209607200

Srikumar M. Raja‡§, Baikun Wang‡, Mandakini Dantuluri¶, Umesh R. Desai¶, Borries Demeler‖, Katharina Spiegel, Sunil S. Metkar‡, and Christopher J. Froelich‡§**

*From the ‡Department of Medicine, Evanston Northwestern Healthcare Research Institute, Evanston, Illinois 60201, the ¶Department of Medicinal Chemistry, Virginia Commonwealth University, Richmond, Virginia 23298, the ‖Department of Biochemistry, University of Texas Health Science Center at San Antonio, San Antonio, Texas 78229, and the **Department of Biochemistry, Molecular Biology and Cell Biology, Northwestern University, Evanston, Illinois 60208*

We have recently shown that the physiological mediator of granule-mediated apoptosis is a macromolecular complex of granzymes and perforin complexed with the chondroitin-sulfate proteoglycan, serglycin (Metkar, S. S., Wang, B., Aguilar-Santelises, M., Raja, S. M., Uhlin-Hansen, L., Podack, E., Trapani, J. A., and Froelich, C. J. (2002) *Immunity* 16, 417–428). We now report our biophysical studies establishing the nature of granzyme B-serglycin (GrB·SG) complex. Dynamic laser light scattering studies establish that SG has a hydrodynamic radius of ~140 ± 23 nm, comparable to some viral particles. Agarose mobility shift gels and surface plasmon resonance (SPR), show that SG binds tightly to GrB and has the capacity to hold 30–60 GrB molecules. SPR studies also indicate equivalent binding affinities (K_d ~ 0.8 μM), under acidic (granule pH) and neutral isotonic conditions (extra-cytoplasmic pH), for GrB·SG interaction. Finally, characterization of GrB·SG interactions within granules revealed complexes of two distinct molecular sizes, one held ~4–8 molecules of GrB, whereas the other contained as many as 32 molecules of GrB or other granule proteins. These studies provide a firm biophysical basis for our earlier reported observations that the proapoptotic granzyme is exocytosed predominantly as a macromolecular complex with SG.

Granzymes and perforin (PFN)[1] have long been recognized as the major components of the lymphocyte granule-mediated apoptosis pathway. However, the molecular details regarding the mechanism of its action are far from clear. A third component of the system, which has received very little attention, is the lymphocyte granule proteoglycan, serglycin (SG). Granzymes and perforin are presumed to exist within the cytoplasmic granules as an ionically linked macromolecular complex with this proteoglycan. The primary amino acid sequence reveals that granzymes as well as perforin are highly cationic and, therefore, would predictably have a strong interaction with the highly anionic sulfated glycosaminoglycan side chains of the granule proteoglycan. We have recently shown that granzyme B (GrB) is exocytosed as a macromolecular complex with serglycin and not in a free form (1). Using *in vitro* reconstituted GrB·SG complex as a model system, we demonstrated that the macromolecular complex can be endocytosed into target cells and induce apoptosis, when delivered by perforin. In addition to GrB·SG, the involvement of proteoglycan-protease complexes in biological processes has been documented for other proteases, including mast cell tryptase and chymase (2–6), matrix metalloproteinase-7 (also known as matrilysin) (7), and cathepsin K (8).

We had initially shown that target cells bind and internalize membrane-bound granzyme and speculated that delivery of the granzyme to the cytosol was dependent on uptake of membrane remnants carrying PFN pores (9). The granule-mediated cell death pathway appears, however, to share a greater similarity to viral-mediated cellular penetration than initially anticipated. A macromolecular granule complex consisting of granzymes, serglycin (SG), and PFN, analogous to a viral particle, may be the central effector. The granule-associated proteoglycan SG contributes to granule-mediated apoptosis by acting as a carrier, which facilitates internalization of GrB and/or PFN. Accordingly, the killer cell is predicted to secrete the macromolecular complex into the synapse-like space between effector and target cell. The complex then binds to the target cell and undergoes endocytosis. Within the acidic vesicle, PFN alters the endocytic membrane facilitating release of the granzyme complex to the cytosol. Although the current understanding of granzyme B/perforin mediated apoptosis pathway in target cells has come from *in vitro* studies using free granzyme and perforin, our recent data make a compelling case that the macromolecular complex of granzyme B with serglycin, and not free cationic granzyme B, is the physiological form involved in the induction of apoptosis in target cells. The implication of this finding is enormous, necessitating re-evaluation of reported molecular events underlying this crucial host defense process, including the mechanism of internalization of GrB in its physiological form as a complex with SG, the mechanism of release of the complex from endocytic vesicles, as well as the subsequent physiological intracellular targets accessed in the complexed form of this protease.

A clear understanding of the mechanism of granzyme B-mediated apoptosis, can only be achieved by understanding the molecular nature of the macromolecular complex. Following up on our most recent work, which shows that the macromolecular

* This work was supported by Grant 5RO1AI04494-03 and a National Arthritis Foundation Biomedical Grant (to C. J. F.), by National Science Foundation Grant DBI-9974819 (to B. D.), and by American Heart Association Grant 0256286U. The costs of publication of this article were defrayed in part by the payment of page charges. This article must therefore be hereby marked "*advertisement*" in accordance with 18 U.S.C. Section 1734 solely to indicate this fact.

§ To whom correspondence may be addressed: Evanston Northwestern Healthcare Research Institute, 2650 Ridge Av., Evanston, IL 60201. Tel.: 847-570-7660; Fax: 847-570-8025; E-mail: c-froelich@northwestern.edu (C.J.F.) or s-raja@northwestern.edu (S. M. R.).

[1] The abbreviations used are: PFN, perforin; AD, adenovirus; CS, chondroitin sulfate; GAG, glycosaminoglycan; GrB, granzyme B; SG, serglycin; SA, streptavidin; SPR, surface plasmon resonance; HRP, horseradish peroxidase; mAb, monoclonal antibody; PVDF, polyvinylidene difluoride; IETD-*p*NA, Boc-Ile-Glu-Thr-Asp-*p*-nitroanilide; FITC, fluorescein isothiocyanate.

GrB·SG complex is the physiological form of GrB involved in granule apoptosis (1), we now report our findings that give an insight into the biochemical nature of the complex, which include the characterization of the proteoglycan, the stoichiometry of the complexes, the affinity of interaction of granzyme B with SG, and the pH dependence of the interaction.

MATERIALS AND METHODS

Cell Lines—The human natural killer lymphoma cell line YT was maintained in bulk culture by using 3 liters bioreactors with Iscove's modified Dulbecco's medium supplemented with 2 mM L-glutamine, 100 units/ml penicillin, 100 μg/ml streptomycin, 5% fetal bovine serum, and 5% Cosmic calf serum (HyClone, Logan, UT).

Reagents—All reagents of highest purity were purchased from Sigma Chemical Co. (St. Louis, MO). Tissue culture supplies were from either Sigma or Invitrogen. The endoglycosidases chondroitinase ABC, heparinase, heparitinase, as well as glycosaminoglycans, were from Seikagaku Corp. (Tokyo, Japan). Proteoglycan molecular weight standards, aggrecan and biglycan from bovine articular cartilage, were obtained from Sigma, whereas chondroitin sulfate was obtained from Seikagaku Corp. Gelcode Blue stain reagent was obtained from Pierce (Rockford, IL). HRP-rat anti-mouse kappa-chain mAb was acquired from Accurate Chemical Scientific Corp. (Westbury, NY). Ready gels (10%, 15%, and 4–15% gradient gels), Silver stain kit, and Immunblot and Sequiblot-PVDF membranes were purchased from Bio-Rad (Hercules, CA). The ECL Western blotting analysis system and Hyperfilm ECL were purchased from Amersham Biosciences (Piscataway, NJ).

Experimental Conditions and Analytical Methods—All experiments were done in 20 mM HEPES buffer, pH 7.4, containing 150 mM NaCl, at room temperature, unless otherwise noted. For experiments at acidic pH, 50 mM NaAc buffer adjusted to pH 5.4 and containing 25 mM NaCl was used. Agarose gel analysis of SG was done as previously described (1). Essentially, the samples were then run on a 1% agarose gel prepared and run in Tris-borate-EDTA buffer, pH 8.3, followed by staining with 0.02% toluidine blue in 3% acetic acid then destaining in 3% acetic acid. SDS-PAGE analysis was performed according to the procedure of Laemmli (10).

Isolation of GrB and SG—Human GrB was isolated as previously described (11). GrB concentrations were based on its absorbance at 280 nm. The extinction co-efficient was calculated from the published sequence, using the procedure described by Gill and von Hippel (12). Human serglycin (SG) was isolated from conditioned media of natural killer cell line YT-INDY as described previously (13). SG was quantitated in terms of its GAG content by Azure A assay (14), with a slightly modified protocol as described below.

Esterolytic Activity of Granzyme B Using IETD-pNA—GrB esterolytic activity was measured using Boc-Ile-Glu-Thr-Asp-*p*-nitroanilide (IETD-*p*NA) as described in (1). Essentially, the rate of hydrolysis of IETD-*p*NA (200 μM) by GrB samples at concentrations ranging from 5 to 50 nM in a total volume of 200 μl, was measured spectrophotometrically using a SpectraPlus V_{max} (Molecular Devices, Sunnyvale, CA) plate reader, in 96-well plates.

Proteoglycan Quantitation—We used a quantitative dye-binding assay for analysis of sulfated glycosaminoglycans and proteoglycans, using a slightly modified protocol described by Thuy and Nyhan (14). Essentially, a standard curve was generated using varying concentrations of standard chondroitin sulfate, ranging from 0 to 2.5 μg/ml. CS standards as well as the SG sample, whose concentration was to be determined, were incubated with a solution of Azure A in water, having an $A_{635} \sim 1.0$. Binding of Azure A to CS results in a decrease in A_{635}, which is proportional to the GAG concentration. The plot of A_{635} *versus* GAG concentration shows a linear dependence with a negative slope, corresponding to the absorbance change per microgram/ml GAG. The concentration of the sample can then be calculated from the decrease in A_{635}. The concentration of CS or SG, described in the text, is in terms of its GAG content.

Enzymatic Digestions of Proteoglycans—Purified proteoglycans were resuspended in either chondroitinase buffer (40 mM Tris-HCl, 40 mM sodium acetate, pH 8.0) or heparinase/heparitinase buffer (100 mM sodium acetate, 10 mM calcium acetate, pH 7.0). Samples were digested with 0.5 unit/ml chondroitinase ABC at 37 °C overnight or with 0.02 unit/ml of heparinase or heparitinase. These digestions were carried out at 37 °C and 43 °C overnight, respectively. The samples were analyzed either on a 4–15% gradient SDS-PAGE, 1% native agarose gels, or on capillary electrophoresis.

Deglycosylation by Alkaline Elimination—The SG dissolved in distilled water was treated with 0.5 M NaOH overnight at 4 °C. The GAG chains and oligosaccharides were liberated from the core peptide by mild alkaline treatment with sodium borohydride (15). The samples were dialyzed against water before capillary electrophoresis analysis.

Isolation and Solubilization of Enriched Cytotoxic Granules for the Analysis of Intact GrB·SG Complexes—Cells (YT, 1×10^6/ml) grown in Iscove's modified Dulbecco's medium containing 5% fetal bovine serum and 5% fetal calf serum at 37 °C were incubated with for 20–24 h. Cytotoxic granules were isolated from the YT cells essentially as described earlier (11). The granule fractions were then solubilized with Zwittergent 3–12 (0.5%, overnight). The insoluble membrane fraction was separated from the soluble fraction by centrifugation at 14,000 rpm in a microcentrifuge. The GrB activity of supernatant was measured by IETD-*p*NA activity. The sample was subjected to size-exclusion membrane filtration using Microcon YM-100 (100-kDa exclusion) (Millipore, Bedford, MA) as earlier reported (1). The retentate sample was then analyzed on a 1% agarose gel under native conditions, along with *in vitro* generated GrB·SG complexes, containing varying ratio of GrB·SG (as described below). This step was followed by transfer onto a PVDF membrane, and the GrB·SG complexes were detected by Western analysis using anti-GrB mAb. Free GrB and SG_{biotin} were also run for comparison. SG_{biotin} was detected by probing with streptavidin-HRP.

Generation of in Vitro GrB·SG Complexes—GrB·SG complexes were prepared by mixing isolated GrB and SG in 20 mM HEPES, pH 7.4, containing 150 mM NaCl. Mixtures were placed on ice for 20 min followed by centrifugal ultrafiltration through a membrane with a 100-kDa exclusion limit (Microcon YM-100, Millipore, Bedford, MA). The choice of membrane was dependent on the observation that GrB exits only in monomeric form (32 kDa) and thus would be retained by the membrane if complexed to the proteoglycan. The mixtures were spun until the controls lacked retentates. The concentrations of GrB, in the retentate (*i.e.* complexes) and in the filtrate, were measured using hydrolysis of the chromogenic substrate, IETD-*p*NA.

Capillary Electrophoresis—Capillary electrophoresis was performed using an automated Beckman MDQ Pace electrophoresis system. Uncoated fused silica capillaries with 50-μm internal diameter and 50-cm length were from Beckman. Electrophoresis buffer consisted of 20 mM sodium borate buffer, pH 8.8, containing either 50 mM boric acid (16) or 50 mM SDS (17). A new capillary was rinsed sequentially with ~5 capillary volumes each of 0.5 M NaOH, distilled, deionized water and finally with electrophoresis buffer before use. This rinse sequence was also used for periodic regeneration of the capillary. The sample was injected using pneumatic pressure to give a capillary plug volume of ~2–5%. Sample concentrations ranged from 1 to 5 mg/ml. Electrophoresis was performed using a constant voltage of 5, 7, or 10 kV, in the normal polarity mode. A UV-visible detector consisting of a filter at either 214 or 280 nm was used to collect the changes in absorbance of electrophoresis buffer passing through a 2-mm window. A data collection frequency of 4 Hz was found sufficient to obtain good electropherograms. The inter-day variation in migration time was ~10%.

Analytical Ultracentrifugation Studies on Isolated SG—Sedimentation velocity studies, on purified SG preparations, were performed using two-channel Epon centerpieces on a Beckman Coulter XL-A analytical ultracentrifuge. SG samples were run in 20 mM HEPES buffer, pH 7.4, containing 150 mM NaCl. SG at three different concentrations of A_{260} of 0.3, 0.5, and 0.7, corresponding to ~15, 20, and 25 μg/ml, in terms of GAG content, were used. Experiments were performed at 20 °C and 35,000 rpm. The rotor with protein sample was equilibrated in the centrifuge to 20 °C in vacuum before each run was started. Velocity data were collected in continuous scan mode with a step size of 0.003 cm at 260 nm. Data editing, van Holde-Weischet analysis (18), and finite element analysis (19) were performed using UltraScan version 5.0.[2] Sedimentation coefficients, diffusion coefficients, and molecular weights were corrected for water at 20 °C as reported by UltraScan.

Dynamic Laser Light Scattering Analysis of SG—Particle size distribution and hydrodynamic radii of SG and GrB·SG complexes were estimated using dynamic laser light scattering, in which one measures the temporal fluctuations of the intensity of light scattered by a sample. Measurements were made using the BIC-200SM goniometer equipped with a 400-channel BI-9000AT digital autocorrelator and photon counter (Brookhaven Instruments Corp., Holtsville, NY). The last eight channels were used for baseline correction. A laser beam of light at 514.5 nm, delivered by a 3-watt argon-ion laser wavelength, was used.

[2] Demeler, B. (2001) An integrated data analysis software package for sedimentation experiments, University of Texas Health Science Center at San Antonio, Department of Biochemistry, available at www.ultrascan.uthscsa.edu.

Samples of SG at a concentration of 40 μg/ml (based on GAG content), in 200 μl, were used for scattering experiments. Prior to measurements, the samples were subjected to microcentrifugation to ensure separation of any particulate matter that might interfere in the analysis. The digital autocorrelation data acquired was analyzed using the Dynamic Light Scattering software, to derive the particle size distribution. The polydispersity within the sample was assessed by analyzing the data using the non-negative least-squares (21) or CONTIN (22) algorithms supplied with the instrument software.

Analysis of Stoichiometry of Interaction of GrB with CS and SG Complexes by Agarose Gel Electrophoresis—The stoichiometry of interaction of GrB with CS or SG was analyzed on a native 1% agarose gel, by exploiting the shift in mobility of the complexes based on an effective change in the mass as well as charge of the complexes. Briefly, complexes were prepared under the conditions of fixed GrB and varying SG or CS concentrations as well as fixed SG or CS and varying the GrB concentrations. Serial 2-fold dilutions of either SG/CS or GrB were prepared and then mixed with a fixed concentration of GrB or SG/CS, in 20 mM HEPES, 150 mM NaCl, pH 7.4, and incubated for 30 min at room temperature. The complexes were then analyzed on a 1% agarose gel (prepared and added to Tris-Borate-EDTA buffer and adjusted to pH 7.4), stained with 0.02% toluidine blue in 3% acetic acid, destained in 3% acetic acid, and subsequently counterstained with Coomassie Blue (Gelcode).

Derivatization of GAGs with Biotin and Quantitation of Biotinylation—Purified SG as well as GAGs were derivatized with biotinamidocaproylhydrazide according to the procedure described in a previous study (23). Biotin-labeled SG and GAGs were separated from unreacted material by Superose-6 gel-filtration chromatography. Derivatization was confirmed by Western blot analysis of labeled material, which was analyzed on an agarose gel, transferred onto a PVDF membrane, and probed using streptavidin-HRP. The degree of biotinylation was quantitated by exploiting the fluorescence enhancement of streptavidin-FITC, on biotin binding. Briefly, a standard curve was generated using a fixed concentration of streptavidin-FITC (100 nM), incubated with varying concentrations of *d*-biotin (0–400 nM), in a fluorescence microtiter plate. The fluorescence of FITC at 520 nm, following excitation at 495 nm, was measured using a SPECTRAmax GEMINI XS fluorescence plate reader from Molecular Devices (Sunnyvale, CA). The concentration of accessible biotin was estimated from the fluorescence of a mixture of streptavidin-FITC with the labeled SG of GAG.

Biosensor Assays—Surface plasmon resonance studies were performed using the IASys Auto+ instrument (Thermo Labsystems Affinity Sensors, Cambridge, UK) in a dual cuvette. Purified SG was derivatized with biotin-amidocaproylhydrazide essentially as described for biotinylation of heparin (23). SPR studies were performed using a biotin cuvette. Total reaction volumes were typically 50 μl. Streptavidin (10 μg/ml, 500 ng) was first immobilized onto the biotin cuvette. The cuvette contents were replaced with buffer to remove unbound streptavidin. Following three washes, biotinylated SG (10 μg/ml, 500 ng) was added to the streptavidin-coated cuvette. Unbound SG was removed similarly by replacing the contents with buffer. Increasing concentrations of a stock solution of GrB (100–200 μg/ml) were then added to both the sample (immobilized SG) as well as the reference cuvette (streptavidin alone). The data was analyzed using the FastFit and Fastplot software from IASys.

Imaging, Computers, and Software—Images of gels and immunoblots were captured either with a Kodak digital camera or Saphir Ultra 2 flatbed scanner and then exported to Adobe Photoshop 6.0. The images were then placed for final presentation in Adobe Illustrator 9.0 using a Macintosh Power G4 computer.

RESULTS

Isolation and Partial Characterization of the Serglycin Secreted by YT Cells—To characterize the interactions between GrB and SG, particularly the affinity of binding and the number of GrB molecules that can bind each SG, we purified the proteoglycan from YT-INDY cells, a natural killer cell line that appears to contain GrB and PFN bound to SG within cytoplasmic granules. In addition, these cells also constitutively secrete SG into culture medium, providing a convenient resource. We isolated SG from YT cell serum-free supernatants, essentially as described by Oynebraten *et al.* (13) for the purification of SG from a THP monocytic cell line. The purified SG was quantitated in terms of its GAG content using the Azure A dye binding assay (see "Materials and Methods").

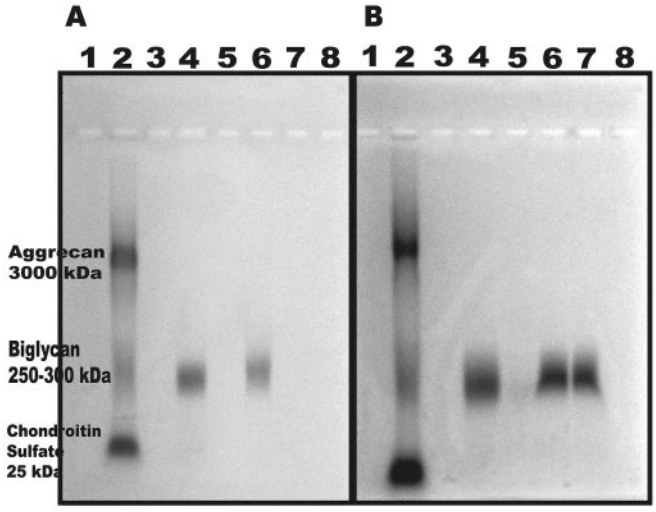

FIG. 1. **Analysis of SG from YT cells.** *A*, agarose gel analysis of purified SG from YT cells. *Lane 2*, molecular mass standards: aggrecan (>3000 kDa), biglycan (250–300 kDa), chondroitin sulfate (~25 kDa); *lane 4*, isolated YT SG; *lane 6*, SG from THP-monocytes. *B*, agarose gel analysis of endoglycosidase digestion of purified SG from YT cells. *Lane 2*, molecular mass standards: aggrecan (>3000 kDa), biglycan (~250–300 kDa), chondroitin sulfate (~25 kDa); *lane 4*, undigested SG; *lane 5*, chondroitinase ABC-digested SG; *lane 6*, heparinase-digested SG; *lane 7*, heparitinase-digested SG.

The isolated SG migrated as a diffuse band in 1% agarose gel with a molecular mass of 200–350 kDa (Fig. 1*A*). The position for SG was comparable to that observed for the previously characterized (13) counterpart from the human monocytic cell line THP-1 (Fig. 1*A*). Endoglycosidase digestion (see Fig. 1*B*) with chondroitinase ABC, heparinase, and heparitinase further confirmed that the protein contained predominantly chondroitin sulfate side chains. The overall characteristics of the isolated PG thus were similar in nature to SG characterized from THP cells (13).

SG, like most other proteoglycans, is heterogeneous due to variations in the number of attached GAGs and their varying chain lengths and degree of sulfation. To assess the heterogeneity of isolated SG as well as isolated CS-GAG chains, we used capillary electrophoresis (CE). CE is a powerful technique widely used for GAG analysis (24). In the normal polarity mode the sample is injected at the anode and detected at the cathode. Under alkaline conditions, the oppositely directed electrophoretic and electro-osmotic forces resolve the species, on the basis of charge to mass (*e*/*m*) ratio. For a polyanionic mixture, the species with the least charge density (*e*/*m*) elutes first, followed by species with increasing charge densities. Homogeneous samples, with a well-defined molecular composition, give sharp peaks, with peak widths of a few seconds, whereas heterogeneous polydisperse samples, including GAGs, elute as broad humps. CE analysis of our isolated SG, showed a broad peak between 50 and 54 min, with a peak width of ~4 min (see Fig. 2*A*), rather than a peak width of a few seconds, indicating that the isolated SG was highly polydispersed. The *inset* in Fig. 2*A* shows the elution monitored at both A_{280} (peptide absorbance) and A_{214} (peptide backbone and sugar residues). CS chains released from the core peptide by base hydrolysis migrated similarly to commercial CS (M_r ~ 25,000) (from *Sturgeon notochord*, Seikagaku Corp., Tokyo, Japan) on an agarose gel (see Fig. 2*B*). This result was confirmed by gel-permeation chromatography on a Superose 6 column (Amersham Biosciences, Piscataway, NJ) (data not shown). The GAG chains released by base hydrolysis of SG also eluted as a broad polydisperse peak at ~18.4 min, in a position similar to intact SG, presumably due to a comparable overall *e*/*m* ratio. When mon-

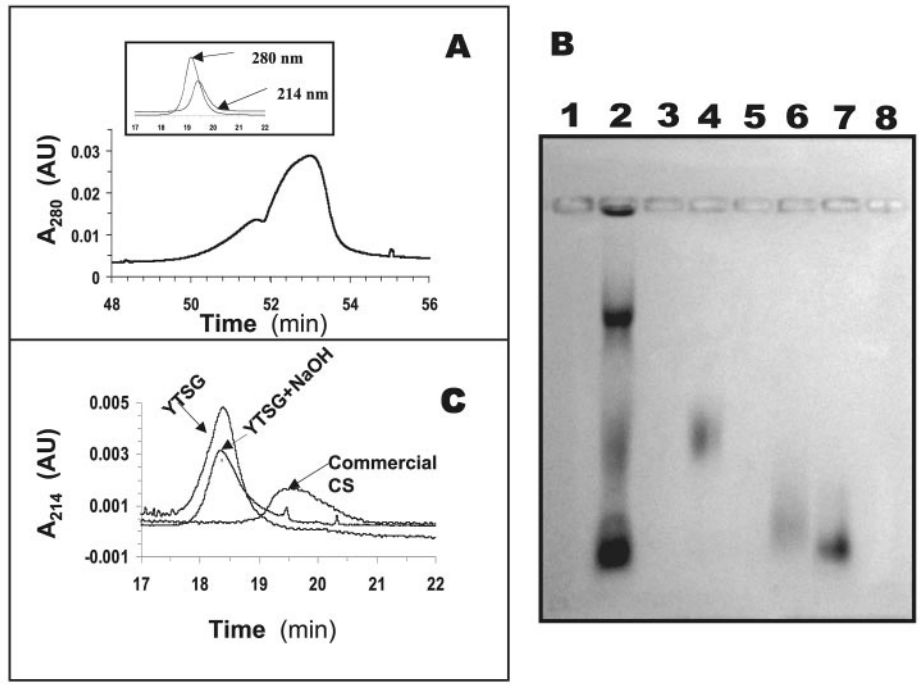

FIG. 2. **Capillary electrophoretic analysis of YTSG and the CS-GAG chain.** *A*, CE run of isolated YTSG. Isolated SG was subjected to a CE analysis, in 20 mM sodium borate buffer, pH 8.8, containing 50 mM SDS, as described under "Materials and Methods." *B*, agarose gel analysis of the base digest of YTSG. *Lane 2*, molecular mass standards: aggrecan (>3000 kDa), biglycan (~250–300 kDa), chondroitin sulfate (~25 kDa); *lane 4*, undigested SG; *lane 6*, NaOH-digested SG; *lane 7*, commercial CS (Seikagaku Corp., Tokyo, Japan). *C*, CE run of NaOH digest of SG. YTSG was subjected to base hydrolysis, and the dialyzed sample analyzed on CE as described under "Materials and Methods."

itored at A_{280}, the sample lacked a discernible peak confirming the signal was due to free GAG and not undigested SG. For comparison we injected commercial CS (from *S. notochord*) as shown in Fig. 2*C*. The elution time for commercial CS (~19.5 min), which was isolated from a non-human source, is a slightly higher retention time (shifted by ~1 min), presumably because of a higher degree of sulfation leading to a greater negative charge and therefore an increased *e/m* ratio.

Analytical Ultracentrifugation and Dynamic Light Scattering Studies on SG—Agarose gel analysis showed that the average molecular mass of isolated SG was 200–350 kDa, similar to our biglycan standard. However, under gel-filtration analysis on a Superose 6 column, SG eluted in the void volume with an estimated molecular mass exceeding 10^6 kDa (data not shown). This difference is likely due to the extended topology of the chondroitin sulfate chains, occupying a much larger molecular volume in the aqueous phase.

Based on differential glycosylation and variance in the total number of GAG chains per core peptide, one can predict significant heterogeneity and polydispersity. To study the molecular size distribution, we performed sedimentation velocity studies on the isolated SG, using various concentrations of the proteoglycan. The van Holde-Weischet distribution plot is shown in Fig. 3*A*. The results indicate that the sample lacks concentration dependence and exhibits substantial heterogeneity due either to heterogeneity in molecular weight, frictional heterogeneity, or, most likely, both. The S value distribution increases from a small S value of around 2 S to more than 25 S.

The molecular weights of the particles can be calculated from Svedberg's law,

$$s/D = [M(1 - \bar{V}^*\rho]/RT \qquad \text{(Eq. 1)}$$

where s is the sedimentation coefficient; D is the diffusion coefficient (given by $D = RT/Nf$, where f is the frictional coefficient); M is the molecular weight; *vbar* is the partial specific volume at experimental temperature T, *rho* is the density of the buffer, and R is the gas constant.

To calculate the M_r of the particles from the s values, knowledge of *vbar* and the diffusion coefficient is necessary. Theoretically, a lower limit may be estimated by assuming that all molecules in the sample sediment into spherical shapes. Based on the method of Cohn and Edsall (25) and as implemented in UltraScan,[2] a *vbar* value of 0.7346 cm^3/g can be safely assumed. However, SG consists predominantly of GAG sugars; therefore, to calculate the M_r distribution of SG, we used a literature value of 0.54 cm^3/g for *vbar*, as reported by Liu *et al.* (26) for isolated GAG chains of another proteoglycan, biglycan. Assuming a *vbar* value of 0.54 cm^3/g and a model of perfect spheres, the largest and fastest sedimenting particle, has a molecular mass of 225 kDa at its lower limit. This value agrees well with the expected molecular weight of SG. The smaller components likely represent the core peptide, which contains fewer numbers and/or shorter lengths of GAG chains attached to it.

To further characterize the hydrodynamic radii and the size distribution of the SG preparation, we used dynamic laser light scattering. The digital autocorrelator was used to determine the autocorrelation function, from which the particle size distribution was derived. Dynamic light scattering measurements further confirmed the polydisperse nature of SG, with particle sizes ranging from ~ 40 to 200 nm (see Fig. 3*B*) and a mean diameter of ~140 ± 23 nm. Therefore, SG appears to occupy a large molecular volume with hydrodynamic radii comparable to certain viral particles. The extended conformation of the GAG chains presumably confers SG with a large surface area and, therefore, the capacity to hold multiple molecules.

Evaluation of the Affinity of Interaction of GrB with SG Using Surface Plasmon Resonance—To quantitate the equilibrium binding affinity of GrB with SG we used surface plasmon resonance (SPR), a technique that measures the binding of a soluble analyte to an immobilized ligand in real-time. Detection is achieved by measuring the changes in the refractive index at the biosensor surface mediated by the biomolecular interaction. SPR has been successfully used to assess the binding interaction of several GAG binding proteins (23, 27, 28).

SG was first biotinylated and purified, and the degree of biotinylation was quantitated as described under "Materials and Methods." Assuming an average molecular mass of 250 kDa for SG, we found that the stoichiometry of biotin labeling was ~19 per SG (data not shown). The binding and dissociation

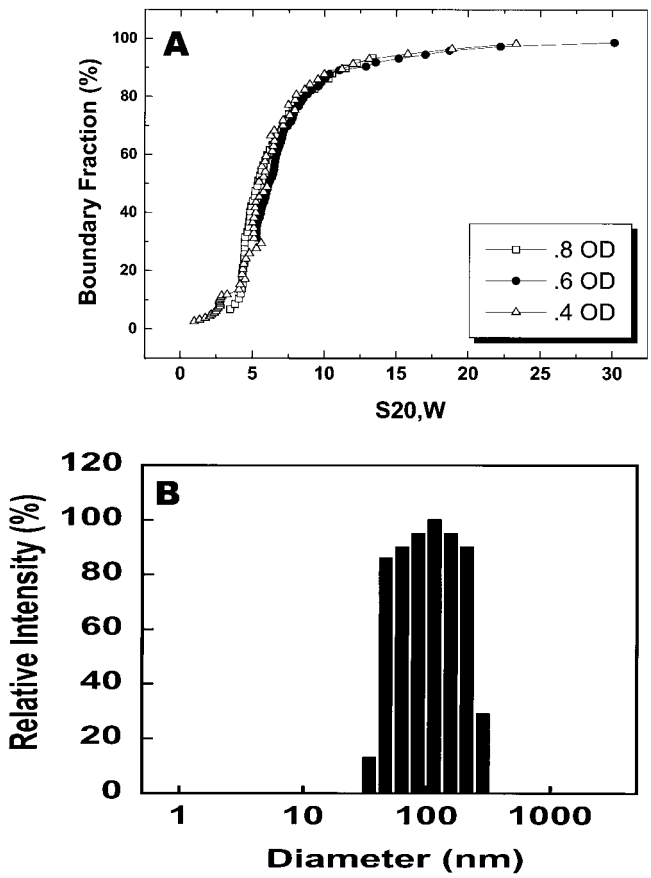

FIG. 3. **Sedimentation velocity and dynamic light scattering analysis of SG.** *A*, SG at three different concentrations were subjected to a sedimentation velocity analysis as described under "Materials and Methods." Shown here is the van Holde-Weischet combined distribution plot. *B*, SG at a concentration of 40.3 μg/ml was subjected to dynamic laser light scattering analysis as described under "Materials and Methods." The autocorrelation function data was analyzed using the CONTIN (22) algorithms supplied with the instrument software. Shown here is the particle size distribution of the SG in the sample.

of GrB to SG was then followed in real-time, by studying the interaction of GrB with SG_{biotin} immobilized onto a streptavidin-coated cuvette surface. Experiments were performed at acidic pH 5.4, to simulate granule conditions, and at pH 7.4, to represent extracellular pH encountered by the complex after exocytosis. Fig. 4*A* shows a typical sensogram for the binding of increasing concentrations of GrB with immobilized SG, at pH 7.4, in the presence of 150 mM NaCl. Addition of GrB resulted in a typical increase in SPR response (measured in response units), which finally reached a plateau when the SG was saturated by the granzyme. The control cuvette showed about 10–15% nonspecific binding to the streptavidin-coated surface. After the association curve reached a plateau, the contents were replaced with buffer to effect dissociation. As seen in Fig. 4*A*, once complexed with SG, there is limited (<15%) dissociation of GrB. Remarkably, as confirmed by the increase in resonance units after dissociation (see Fig. 4*A*), the released granzyme appeared to re-associate. A similar observation was noted for experiments under acidic pH conditions (data not shown).

The association as well as dissociation phase of the sensograms were analyzed, after subtraction of the nonspecific binding. Both association and dissociation phases fitted to a single Langmuir model (A + B $\rightleftarrows$ AB) where the association and dissociation rate constants were derived by non-linear regression analysis of the background subtracted data, using IASys Fastplot software. The slope of the plot of k_{obs} *versus* GrB concentration (Fig. 4*B*) gives the second order association rate constant (k_{on}). The off-rate is then calculated by non-linear regression analysis of the dissociation curves in the sensograms. The ratio of k_{off}/k_{on} gives the equilibrium binding constant (K_d). As seen from Fig. 4*B*, the k_{on} for binding of GrB to SG was $0.34 \pm 0.01 \times 10^6$ M^{-1} s^{-1} at pH 7.4, whereas at pH 5.4 the association rate was ~50% slower ($0.16 \pm 0.01 \times 10^6$ M^{-1} s^{-1}). The dissociation rate for the GrB·SG complex at pH 7.4 was 0.24 ± 0.05 s^{-1}, whereas at pH 5.4 the k_{off} was 0.16 ± 0.04 s^{-1}. The effective K_d was calculated to be 0.71 μM at pH 7.4, whereas at pH 5.4 it was 0.98 μM. The apparent K_d for GrB·SG binding can additionally be calculated from the amplitude data by fitting the observed response units as a function of GrB concentration, to a hyperbola. The plot of the amplitude of the SPR signal on binding of GrB with immobilized SG (in response units) *versus* the GrB concentration is shown in Fig. 4*C*. The apparent K_d values derived from this fit were found to be 0.84 ± 0.09 μM *versus* 0.69 ± 0.17 μM at pH 7.4 and 5.4, respectively. These values agree with results derived from the association and dissociation rates. Overall, the results indicate that GrB has a similar affinity for SG at both pH 5.4 and pH 7.4 providing strong biophysical support for our earlier observation that GrB is secreted predominantly complexed with SG (1).

The SPR data were also used to calculate the stoichiometry of GrB·SG binding. The molar equivalent of immobilized SG was calculated from the response units under the conditions for the binding of SG_{biotin} with the SA-coated cuvette, assuming an average molecular mass of 250 kDa. Similarly, the mole equivalent value of GrB binding to SG was calculated, based on the response units for GrB·SG binding (after background subtraction), using a molecular mass of 32 kDa for GrB. The ratio of the mole equivalents of bound GrB per mole equivalents of immobilized SG gives the stoichiometry of binding. At pH 5.4, the maximal stoichiometry of binding of GrB to SG is ~51 ± 4 molecules per molecule of SG, whereas at pH 7.4 it is ~30 ± 4. The capacity of SG to bind a greater number of GrB molecules at acidic pH as compared with neutral pH may be due to differences in the CS-GAG conformations, exposing more binding sites. We have seen that there is a 10-fold higher binding of SG_{biotin} to the streptavidin-coated surface at pH 5.4, as compared with pH 7.4. This may reflect pH-dependent differences in the conformation of GAG side chains, exposing a greater number of biotin molecules accessible to SG.

Stoichiometry of Binding of Granzyme B with Chondroitin Sulfate and Serglycin Proteoglycan, in Vitro, Using Agarose Gel Electrophoresis—Based on the strongly cationic and anionic charges of GrB and SG, respectively, and the fact the CS-GAG side chains can have an extended topology, one may predict that multiple GrB molecules will bind each CS side chain of SG. To establish the stoichiometry of binding, we analyzed complexes formed by mixing a fixed concentration of GrB with a serially 2-fold-diluted sample of CS or SG and vice versa by evaluating mobility shifts in 1% agarose gels. Free CS or SG, being anionic, migrates toward the anode, whereas free GrB, being cationic, migrates toward the cathode. The binding of GrB to CS or SG results in a decrease in the net negative charge as well as increase in overall mass. The complexes are therefore resolved on the basis of varying mass to charge ratios. The CS or SG was visualized with GAG-reactive toluidine blue O destained with 3% acetic acid and subsequently stained with Coomassie Blue to visualize protein bands.

The results of the interaction of GrB with CS, at fixed concentration of GrB and varying concentration of CS and as well as complementary studies with fixed CS and varying GrB, are shown in Fig. 5 (*A* and *B*). In both cases the GrB:CS ratio varied from 0.25- to 8-fold over CS (w/w). CS can bind up to a 4-fold

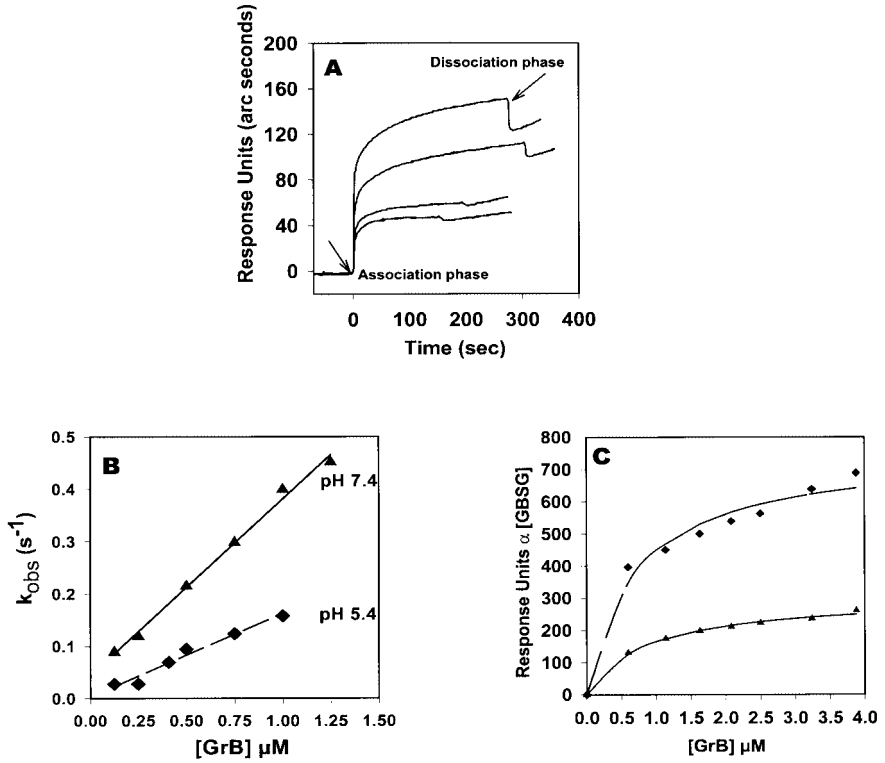

FIG. 4. **Surface plasmon resonance analysis of GrB·SG binding.** *A*, SG_{biotin} was immobilized onto a streptavidin-coated cuvette. Increasing concentrations of GrB from 0.25 to 2 μM were added to the cuvette, and the increase in response units (RU) was measured as a function of time. *B*, the SPR sensograms data, shown in *A*, were subjected to non-linear regression analysis using a single-phase association model. The forward rate constant was derived from the fits of the association phase, whereas the reverse rate constants were derived from the fits of the dissociation phase. Shown here is a plot of the observed forward rate constants as a function of GrB concentration. The second-order association rate constant was derived from the slope of a linear fit of this data. *C*, the amplitude of the SPR change in resonance units, which is a measure of the amount of GrB·SG complex formed at equilibrium, was calculated from the global analysis of the sensograms. The data were fitted to a hyperbola. The maximal extent of GrB binding as well as an apparent K_d value was derived as a parameter of the fit.

excess of GrB (w/w), inferred from the absence of free GrB band migrating toward the anode as well as the appearance of high molecular weight GrB-CS bands. This observation was also supported by the disappearance of the free SG band visualized by toluidine blue O staining (data not shown). At the maximal ratio of GrB to CS of 4:1 (w/w), ~3 molecules of GrB are bound per molecule of CS.

Assuming that an SG molecule (M_r ~ 250,000) contains 10 CS-GAG chains, of which each averages M_r ~25,000, it could be predicted that SG would bind ~30 molecules of GrB. This was exactly what we found when we used this approach to examine the stoichiometry of GrB·SG complexation (Fig. 5, *C* and *D*). The ratio of GrB to SG ranged from 0.5- to 16-fold (w/w). The results indicate that SG can bind about a 4-fold excess of GrB (w/w), or ~32 molecules of GrB per SG molecule assuming an average molecular mass of 250 kDa for SG. In addition, this is in excellent agreement with the numbers derived from SPR analysis. It is worth noting that similar stoichiometries of binding have been predicted for complexes of mast cell tryptases with proteoglycans (4). We attempted a similar analysis under conditions simulating granule pH. However, GrB·SG mixing at acidic pH caused precipitation, which voided the analysis.

Characterization of the GrB·SG Complexes from Granules—Having established agarose gel-shift assays as a method to characterize *in vitro* complexes of GrB·SG, we used this method to characterize the size of GrB·SG complexes from granule extracts of YT-INDY cells. Enriched granule fractions were subjected to dissolution using 0.5% Zwittergent 3–12, the detergent providing optimal solubilization (1). The insoluble membrane fraction was separated from the soluble fraction by centrifugation at 14,000 rpm. For comparison, increasingly saturated *in vitro* complexes of GrB with SG were generated by mixing a fixed concentration of SG with increasing concentrations of GrB. The samples were then analyzed on an agarose gel followed by Western blotting using anti-GrB antibody. For comparison, SG_{biotin} was loaded on the agarose gel along with the other samples (see legend to Fig. 6) and probed using streptavidin-HRP. The results are as shown in Fig. 6. As expected, free GrB moved toward the cathode, while free SG, as well as GrB·SG complexes moved toward the anode. Also, the *in vitro* complexes show a clear mobility shift with increasing amounts of bound GrB. At a 4:1 ratio (w/w), there would be ~32 molecules of GrB per SG, assuming an molecular mass of 250 kDa for SG, whereas at a mass ratio of 1:1, the molar ratio would be 8:1. The GrB·SG complexes from the granule extract (*lane 5*) appear as two bands, possibly containing different stoichiometries of bound GrB, in comparison with the *in vitro* complexes (*lanes 6–8*). The first band appears slightly above SG_{biotin} (*lane 3*) but below GrB·SG with a mass ratio of 1:1 (w/w). It therefore appears to contain less than 8 molecules of bound GrB. The second band appears as a higher molecular weight complex. This may contain an excess of over 4-fold of GrB over SG (> 32 molecules of bound GrB), as compared with the *in vitro* standard (*lane 8*). Alternatively, the larger molecular weight band could represent a complex containing other bound cationic granule proteins. A similar analysis, using an anti-perforin antibody, shows a PFN band in the larger molecular weight band but not the first (smaller molecular weight) band (data not shown). Identification of other SG bound components using proteomics is in progress.

DISCUSSION

Our understanding of the mechanism of granule-mediated apoptosis continues to gain clarity. Originally, perforin was postulated to form pores in the target cell membrane, which acts as a gateway for passive diffusion of granzymes and other cytotoxic molecules into the target cell. Second, although granzymes existed as a complex with proteoglycans within granules, it was assumed that the granzymes dissociated from the proteoglycan after exocytosis entered the target in free form. We have recently shown that perforin has a more enigmatic function than the intuitively simple gateway model (1). Additionally, GrB appears to function as a macromolecular complex with SG and not as the free cationic granzyme (1). We therefore proposed that granule-associated PGs act as a scaffold for gran-

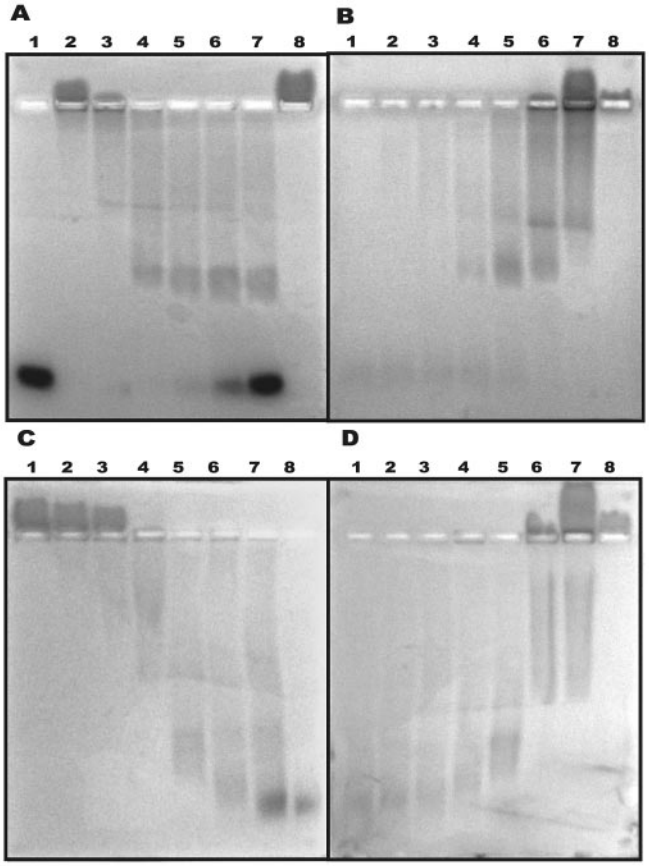

FIG. 5. **Stoichiometry of interaction of GrB with chondroitin sulfate and SG using mobility-shift analysis on an agarose gel.** The stoichiometry of interaction of GrB with CS or SG was analyzed on 1% agarose gel by exploiting the mobility shift of complexes. GrB and CS/SG were allowed to react in a total volume of 15 μl. Serial 2-fold dilutions containing either CS (8 $\rightarrow$ 0.25 μg) (*Panel A*) or GrB (16 $\rightarrow$ 0.5 μg) (*Panel B*) were prepared and mixed with a fixed concentration of GrB (2 μg) or CS (2 μg), respectively, in 20 mM HEPES, 150 mM NaCl, pH 7.4, and incubated for 30 min at room temperature. *Panel A*: *lane 1*, CS; *lanes 2–7*, GrB-CS; *lane 8*, GrB. *Panel B*: *lane 1*, CS; *lanes 2–7*, GrB-CS; *lane 8*, GrB. In a similar design, GrB and SG were allowed to react in a total volume of 15 μl. Serial 2-fold dilutions containing either SG (4 $\rightarrow$ 0.125 μg) (*Panel C*) or GrB (32 $\rightarrow$ 1 μg) (*Panel D*) were prepared and mixed with a fixed concentration of GrB (2 μg) or SG (2 μg), respectively. *Panel C*: *lane 1*, SG; *lanes 2–7*, GrB·SG; *lane 8*, GrB. *Panel D*: *lane 1*, SG; *lanes 2–7*, GrB·SG; *lane 8*, GrB. The complexes were then run on a 1% agarose gel (prepared and run in Tris-Borate-EDTA buffer adjusted to pH 7.4), stained with 0.02% toluidine blue O in 3% acetic acid, destained in 3% acetic acid, and subsequently counterstained with Coomassie blue (Gelcode)

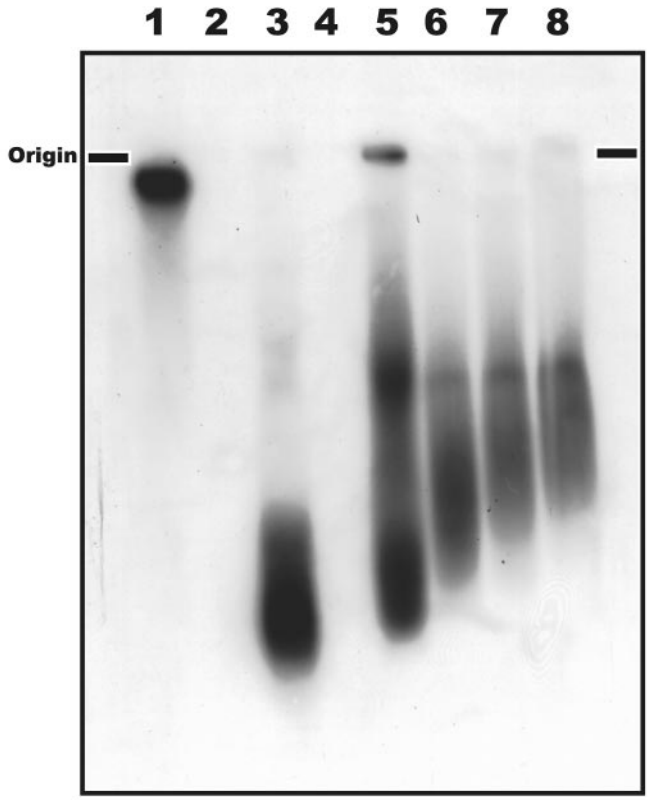

FIG. 6. **Characterization of intact GrB·SG complexes from granules.** Granule extract (*lane 5*), was prepared and analyzed by agarose gel analysis, followed by Western blotting, as described under "Materials and Methods." For comparison GrB (*lane 1*), SG_{biotin} (*lane 3*), and *in vitro* GrB·SG complexes at ratios of 1:1, 2:1, 4:1, and (w/w) (*lanes 6–8*, respectively) were run.

ular components modulating enzymatic activities and ensuring precise intracellular targeting. The studies described in this report are the first step toward understanding the biophysical interactions of granzymes, perforin and SG, which are the molecular effectors of granule-mediated apoptosis.

SG is secreted by various hematopoietic cells, including cytotoxic T-lymphocytes (29). We have confirmed that the granule-associated proteoglycan in cytotoxic cells, as well as that secreted by YT-cells, is identical to the chondroitin-sulfate proteoglycan, SG. Furthermore, we have documented the heterogeneous and polydisperse nature of this proteoglycan and shown that, although the average molecular mass is about 250,000 Da, the proteoglycan has a large molecular volume with a hydrodynamic radius comparable to some virions. The enormous size and the negatively charged surface and extended GAG-chain conformation in solution offer an ideal scaffold to sequester multiple copies of various cationic granule components. However, dependence of the affinity and stoichiometry of granule components on pH defines whether a molecule remains bound to SG after exocytosis. Having reported that secreted GrB was complexed with SG, it was necessary to further characterize this interaction by quantifying the strength of the association, the number of granzyme molecules that bound each SG, and the size of complexes within the granules.

The association/dissociation profiles and the derived K_d readily demonstrate the tight binding of GrB to the CS-GAGs of SG and emphasize the tendency of dissociated molecules to re-associate (Fig. 4*A*). Changes in the pH-dependent affinity of a granule component for SG could predict whether a component dissociates or remains bound after exocytosis. A component that has a weaker K_d at extracellular than at granule pH may be expected to dissociate during a shift to neutral pH. A comparison of the K_d values derived from SPR as a function of pH clearly shows that GrB has a similar affinity for SG under both conditions. This observation, coupled with the minimal dissociation of GrB from SG, once bound, validates our observation that lymphokine-activated killer cells secrete GrB as a complex with SG (1).

The capacity of the SG scaffold to bind multiple GrB molecules was evident from the SPR and mobility shift data. SG could bind as many as 30 molecules of GrB at neutral pH and 50 molecules at acidic. Nevertheless, although SG had the capacity to bind between upwards to 50 molecules of GrB *in vitro*, it is unlikely that the stoichiometry of GrB·SG would be this high *in vivo*. The granule-proteoglycan composition would depend on the number of different granule components (granzymes, perforin, granulysin, chemokines, etc.) competing for the anionic binding sites. Wagner *et al.* (20) have reported that

β-chemokines are also secreted by human immunodeficiency virus type 1-specific cytotoxic T-lymphocyte granules as a complex with proteoglycans. We plan to gain a more detailed understanding of the granule·proteoglycan complexes from cytotoxic cells by performing similar biophysical studies on the interaction of other isolated cationic granule-proteins, including various granzymes, perforin, granulysin, and chemokines (RANTES (regulated on activation normal T cell expressed and secreted), MIP-1α, and MIP-1β) with SG.

Having characterized the nature of GrB·SG interaction reconstituted *in vitro*, we sought to compare the molecular size of GrB·SG obtained from granules. Our analysis revealed two forms. The lower molecular weight form was comparable in size to SG containing less than 8 GrB molecules, whereas the higher form was comparable to SG containing the equivalent of 32 GrB molecules (see Fig. 6). Both molecular forms, as discussed above, likely contain other granule proteins; therefore, we are currently identifying these components by proteomics.

In conclusion, we believe that further characterization of granule-associated complexes will provide a clearer understanding of the mechanism underlying granule-mediated apoptosis. This form of cell death represents a phenomenon where the target cell internalizes a multimeric effector (SG, PFN, and multiple granzymes) and simultaneously engages multiple death pathways. Most importantly, this macromolecular complex may be viewed as nature's design for a modular drug delivery system. The proteoglycan, SG, acts as a scaffold holding the components necessary for efficient delivery and signaling: PFN acts as translocator, whereas granzymes are executioners. Consequently, an understanding of the mechanism of cell-death induced by this complex should assist in the design of therapeutics based on this multimeric complex, with SG as the scaffold, which can support the targeting (disease cell-specific) translocating (endosomolytic) and executioner modules (granzymes).

Acknowledgments—Surface plasmon resonance, analytical ultracentrifugation, and dynamic laser light scattering studies were done at the Keck Biophysics facility, established in the Department of Biochemistry, Molecular Biology and Cell Biology, Northwestern University and funded by the W. M. Keck foundation. We thank Dr. Phillip Bird, Monash University, Australia, for critical comments on the manuscript. We also thank Qing Qing Zhen and Alina Huang for their technical assistance.

REFERENCES

1. Metkar, S. S., Wang, B., Aguilar-Santelises, M., Raja, S. M., Uhlin-Hansen, L., Podack, E., Trapani, J. A., and Froelich, C. J. (2002) *Immunity* **16,** 417–428
2. Goldstein, S. M., Leong, J., Schwartz, L. B., and Cooke, D. (1992) *J. Immunol.* **148,** 2475–2482
3. Matsumoto, R., Sali, A., Ghildyal, N., Karplus, M., and Stevens, R. L. (1995) *J. Biol. Chem.* **270,** 19524–19531
4. Pejler, G., and Berg, L. (1995) *Eur. J. Biochem.* **233,** 192–199
5. Lindstedt, L., Lee, M., and Kovanen, P. T. (2001) *Atherosclerosis* **155,** 87–97
6. Pejler, G., and Maccarana, M. (1994) *J. Biol. Chem.* **269,** 14451–14456
7. Yu, W. H., and Woessner, J. F., Jr. (2000) *J. Biol. Chem.* **275,** 4183–4191
8. Li, Z., Hou, W.-S., and Bromme, D. (2000) *Biochemistry* **39,** 529–536
9. Froelich, C. J., Orth, K., Turbov, J., Seth, P., Gottlieb, R., Babior, B., Shah, G. M., Bleackley, R. C., Dixit, V. M., and Hanna, W. (1996) *J. Biol. Chem.* **271,** 29073–29079
10. Laemmli, U. K. (1970) *Nature* **227,** 680–685
11. Hanna, W. L., Zhang, X., Turbov, J., Winkler, U., Hudig, D., and Froelich, C. J. (1993) *Protein Expr. Purif.* **4,** 398–404
12. Gill, S. C., and von Hippel, P. H. (1989) *Anal. Biochem.* **182,** 319–326
13. Oynebraten, I., Hansen, B., Smedsrod, B., and Uhlin-Hansen, L. (2000) *J. Leukoc. Biol.* **67,** 183–188
14. Thuy, L. P., and Nyhan, W. L. (1992) *Clin. Chim. Acta* **212,** 17–26
15. Park, Y., Yu, G., Gunay, N. S., and Linhardt, R. J. (1999) *Biochem. J.* **344,** 723–730
16. al-Hakim, A., and Linhardt, R. J. (1991) *Anal. Biochem.* **195,** 68–73
17. Desai, U. R., Wang, H., Ampofo, S. A., and Linhardt, R. J. (1993) *Anal. Biochem.* **213,** 120–127
18. van Holde, K. E., and Weischet, W. O. (1978) *Biopolymers* **17,** 1387–1403
19. Demeler, B., and Saber, H. (1998) *Biophys. J.* **74,** 444–454
20. Wagner, L., Yang, O. O., Garcia-Zepeda, E. A., Ge, Y., Kalams, S. A., Walker, B. D., Pasternack, M. S., and Luster, A. D. (1998) *Nature* **391,** 908–911
21. Lawson, C. L., and Hanson, R. J. (1974) *Solving Least Squares Problem*, Prentice-Hall, Englewood Cliffs, NJ
22. Provencher, S. W. (1982) *Comput. Phys. Commun.* **27,** 229–242
23. Martin, L., Blanpain, C., Garnier, P., Wittamer, V., Parmentier, M., and Vita, C. (2001) *Biochemistry* **40,** 6303–6318
24. Mao, W., Thanawiroon, C., and Linhardt, R. J. (2002) *Biomed. Chromatogr.* **16,** 77–94
25. Cohn, E. J., and Edsall, J. T. (1943) *Proteins, Amino Acids and Peptides as Ions and Dipolar Ions*, Reinhold Publishing Corp., New York
26. Liu, J., Laue, T. M., Choi, H. U., Tang, L. H., and Rosenberg, L. (1994) *J. Biol. Chem.* **269,** 28366–28373
27. Rathore, D., McCutchan, T. F., Garboczi, D. N., Toida, T., Hernaiz, M. J., LeBrun, L. A., Lang, S. C., and Linhardt, R. J. (2001) *Biochemistry* **40,** 11518–11524
28. Seet, B. T., Barrett, J., Robichaud, J., Shilton, B., Singh, R., and McFadden, G. (2001) *J. Biol. Chem.* **276,** 30504–30513
29. Toyama-Sorimachi, N., Kitamura, F., Habuchi, H., Tobita, Y., Kimata, K., and Miyasaka, M. (1997) *J. Biol. Chem.* **272,** 26714–26719